Eur. J. Mineral.
2003, **15**, 1007–1018

Pertsevite, a new silicatian magnesioborate mineral with an end-member composition Mg_2BO_3F, in kotoite marble from east of Verkhoyansk, Sakha-Yakutia, Russia

WERNER SCHREYER[1]*, THOMAS ARMBRUSTER[2], HEINZ-JÜRGEN BERNHARDT[1] and OLAF MEDENBACH[1]

[1] Institut für Geologie, Mineralogie und Geophysik, Ruhr-Universität, D-44780 Bochum, Germany
* Corresponding author, e-mail: werner.schreyer@ruhr-uni-bochum.de
[2] Laboratorium für chemische und mineralogische Kristallographie, Universität Bern, Freiestrasse 3, CH-3012 Bern, Switzerland

Abstract: Pertsevite is a new Mg borate from a contact-metasomatic kotoite marble from the region east of Verkhoyansk, Sakha-Yakutia, northeastern Siberia. The end member is defined as Mg_2BO_3F, which is the composition of a synthetic phase. The natural material consistently contains from 4 to 12 wt.% SiO_2 as well as some OH. This is due to the substitutions Si + O for B + F and OH for F. A representative composition, which is an intermediate member of a solid solution series $Mg_2BO_3(F,OH) - Mg_2SiO_4$, has the composition (EMP data, OH calculated for charge balance) SiO_2 8.25; Al_2O_3 0.10; B_2O_3 22.44; FeO 3.71; MnO 0.65; MgO 57.39; CaO 0.24; F 7.29; H_2O_{calc} 1.67; total 98.97 wt.%, corresponding to $(Mg_{1.88}Fe^{2+}_{0.07}Mn_{0.01})(B_{0.85}Si_{0.18})O_{3.21}F_{0.54}(OH)_{0.24}$ or simply $Mg_2(B_{0.8}Si_{0.2})O_{3.2}(F,OH)_{0.8}$. A general formula of silicatian pertsevite may be given as $Mg_2(B,Si)O_3(F,OH,O)$. Like the synthetic end member Mg_2BO_3F, silicatian pertsevite is orthorhombic, space group $Pna2_1$, with $a = 20.490(6)$, $b = 4.571(1)$, $c = 11.890(3)$ Å, $V = 1113.61(5)$ Å^3, Z = 16 and $D_{calc} = 3.12$ g/cm^3 for the above composition. Its structure is based on a hexagonal close-packed arrangement of anions similarly as for forsterite, but with cations occupying different sets of voids. BO_3 triangles are randomly replaced by SiO_4 tetrahedra with Si lying outside of the planes defined by the BO_3 triangles. The crystals are colorless in thin section, biaxial (+) with (for the above composition) $\alpha = 1.609(1)$, $\beta = 1.620(1)$, $\gamma = 1.642(1)$ for 589 nm, $2V_{Z\,meas} = 65(1)°$ and no visible dispersion. In the one thin section of the kotoite marble available, pertsevite occurs as anhedral crystals interspersed with calcite, kotoite, forsterite, clinohumite, spinel, ludwigite and a new member of the hulsite group. Based on analytical data, but also on structural considerations, there is a large miscibility gap between silicatian pertsevite and practically boron-free forsterite. Pertsevite is probably more widespread than this single example suggests; its being overlooked may be explained by its close resemblance to forsterite and humite group minerals in thin section.

Key-words: new mineral: pertsevite, magnesioborate, chemical analysis (mineral), solid solution, crystal structure, kotoite marble, Siberia.

Introduction

Dr. N.N. Pertsev, Moscow, provided us with a thin section, in which he suspected, rightly so, a new mineral of the hulsite group (Pertsev *et al*., submitted). During our petrographic and electron microprobe investigations at Bochum, the coexisting mineral assemblage of the enclosing kotoite marble was studied as well. Surprisingly, among the less spectacular minerals expected to be Mg-silicates such as forsterite and members of the humite-group, a phase was discovered that exhibited unusually low, but variable amounts of silicon in addition to magnesium and fluorine. However, the analytical totals were so low that a major component of this phase was obviously missing. More detailed electron microprobe work showed, at first qualitatively, that the missing component was B_2O_3 in considerable quantities. It was not until boron could be determined quantitatively, that cation ratios were approximated. On this basis, we suspected first the unknown phase to represent strongly boron-bearing members of the humite group, or else, a strongly borian forsterite. Even when neglecting silicon, no known Mg-borate mineral such as fluoborite could be named with relevant cation ratios.

The solution of the problem, which is to be presented here in detail, came after one of us (O.M.) succeeded in separating from the thin section a minute flake of the unknown phase, which could be used for a crystal structure determination. The result was that the new mineral is a silicon-bearing derivative of the synthetic phase α-Mg_2BO_3F, for which the crystal structure had been determined by Brovkin & Nikishova (1975). A first account on the properties of the new mineral was given in an abstract for the 2002 IMA-Meeting

DOI: 10.1127/0935-1221/2003/0015-1007
0935-1221/03/0015-1007 $ 5.40

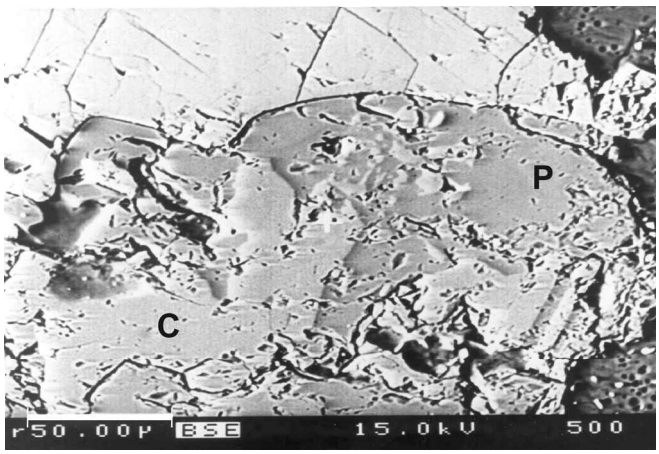

Fig. 1. Backscattered electron (BSE) picture of pertsevite (P, darker grey) partially replacing clinohumite (C, lighter grey). The still lighter grey mineral with cleavage at the top contacting only pertsevite is calcite.

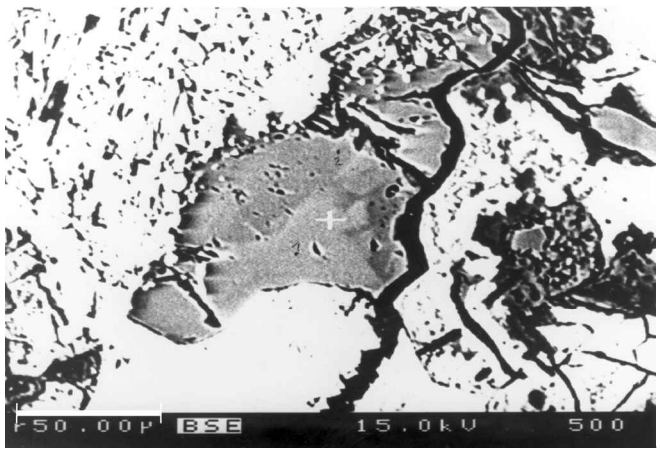

Fig. 2. BSE picture of a chemically heterogeneous crystal of pertsevite (center) in contact with an aggregate of ludwigite needles (to the left). The lighter colored portions of pertsevite (*e.g.* near the center cross) have relatively high Si/B, the darker ones near ludwigite lower Si/B ratios. The homogeneous light-colored phase at the bottom is calcite. On the right-hand side of the picture beyond the crack are fine-grained unidentified products of secondary alteration.

at Edinburgh (Schreyer *et al*., 2002), where pertsevite was called the "potentially new mineral B".

α-Mg_2BO_3F was first reported as a synthetic phase by Grigoriev & Brovkin (1969) along the join sellaite – kotoite in the system $MgO - MgF_2 - B_2O_3$. At atmospheric pressure it is stable below 750° C. However, these same authors could also synthesize the phase hydrothermally at 600° C and an unspecified low pressure.

The new mineral is named after the well-known Russian investigator of boron minerals and deposits, Nikolai Nikolayewich Pertsev, Moscow, who had collected the kotoite marble sample and dedicated the thin section studied. The mineral and its name were approved by the IMA-Commission on New Minerals and Mineral Names (CNMMN-2002-030). Type material has been deposited at the Mineralogical Collection of the Institut für Geologie, Mineralogie und Geophysik, Ruhr-Universität Bochum, Germany, Catalogue Number 25164.

Occurrence

Pertsevite occurs as a newly recognized constituent (about 5-10 %) of a kotoite marble of considerable mineralogical complexity, which also carries a new member of the hulsite group (Pertsev *et al*., submitted). The sample was collected by N. N. Pertsev during 1964 in the basin of the river Yana some 250 km E of Verkhoyansk in what is now the Republic of Sakha-Yakutia in the Russian Federation. The exact locality lies near the mouth of Kebirin`ya creek, a northern tributary of Dogdo river (approximately 67.5° N, 139° E). It is one of many small occurrences of magnesian skarns with boron mineralization that developed widely in contacts of Mesozoic granosyenite massifs, apparently belonging to the Verkhne-Tiryakhtyakh batholith, with Palaeozoic dolomite marbles. The area is part of the extensive Mesozoic belt of Sn-Au-B mineralization of northeastern Asia, which extends as far as northwestern North America (Alaska). Detailed descriptions of the enormous wealth of skarn minerals and rock types in the Siberian part were presented by Pertsev (1971) and, emphasizing hulsite-group minerals and other magnesian borates, by Rudnev (1996) and Aleksandrov *et al.* (2000). More than 20 Ca- and Mg-borate minerals are known from the region. Here are the type localities for sakhaite, borcarite, and olshanskyite. Pertsev (1971, p. 105-106) described the mineral danburite from the very locality of the pertsevite-bearing sample studied here. The kotoite and kotoite marble zones occupy the outermost position within the sequence of magnesian skarns around the granitic intrusions. According to Pertsev *et al*. (submitted) crystallization took place under conditions of low load and fluid pressures, low CO_2 fugacity but widely varying temperatures (from 800° C to several tens of degrees only).

Only the one thin section (no. B-1048) was available for our study, because the original sample could no longer be located. In addition to the new mineral of the hulsite group, alumino-magnesiohulsite (Pertsev *et al*., submitted), and to pertsevite, the following minerals were identified: calcite, kotoite, forsterite, clinohumite, spinel and ludwigite. Secondary minerals of minute grain size mainly replacing kotoite are szaibelyite and brucite, or mixtures thereof. One small grain of löllingite was detected as well.

Electron imaging and optical petrography

Under the polarizing microscope, pertsevite is hard to distinguish at first from the other Mg-rich silicates and borates, except that it often displays – within single grains – highly variable optical interference colors ranging from first-order grey to third-order colors. Its grain boundaries against adjacent minerals often could not be defined visually. Therefore, backscattered electron (BSE) pictures together with energy dispersive qualitative analyses using the electron microprobe were employed to define and select the pertsevite crystals for quantitative chemical analyses. The BSE picture

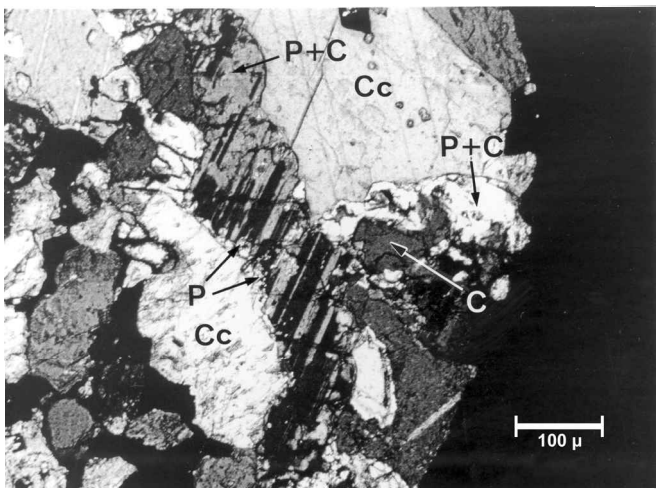

Fig. 3. Photomicrograph of thin section B-1048 using crossed nicols. In the center a large, north-south elongated crystal of twinned clinohumite (C) can be seen, which is peripherally replaced by pertsevite (P). This may partly be recognized, along the left rim of clinohumite by small crystals of P exhibiting higher optical interference (white) than C (grey to black), but also – without any change in interference – by the discontinuation of clinohumite twin lamellae (upper part, P+C). The seemingly homogeneous white area near the right end of the thin section also labelled P+C corresponds to the right-hand portion of the BSE picture of Fig. 1, in which the minerals pertsevite and clinohumite are readily distinguishable. Cc = calcite.

of Fig. 1 shows pertsevite in intimate intergrowth with clinohumite, which is believed to have been partially replaced by pertsevite. In Fig. 2, a chemically inhomogeneous pertsevite crystal is in contact with an aggregate of ludwigite needles.

Once pertsevite had been located by BSE images, optical petrography could be used to define overall textural relationships. In the photomicrograph of Fig. 3, the large clinohumite crystal, here easily recognized by its twinning, is partly surrounded by a fine-grained fabric of pertsevite, which – in this particular orientation – shows mostly lighter colors. However, pertsevite may also be completely masked in the grey, untwinned areas of the upper portion of the clinohumite crystal because of practically identical interference colors. The light-colored, seemingly homogeneous area near the right end of Fig. 3 is identical to part of the BSE picture of Fig. 1, where it manifests itself as a mixture of pertsevite and relics of clinohumite. Note that in such P+C-intergrowths of Fig. 3 the two phases exhibit also identical optical refraction so that no Becke lines appear at their mutual borders. No doubt, these optical properties are the reason why pertsevite has been overlooked thus far. In other places of the thin section, optically heterogeneous, anhedral pertsevite crystals attaining diameters up to 150 micrometers appear independently of other borate and silicate minerals within masses of calcite, or as inclusions in larger calcite crystals together with kotoite. There are also direct grain boundaries of pertsevite against kotoite, which is best recognized by its thin peripheral alteration into szaibelyite and brucite.

Spinel forms independent euhedral crystals, around 100 micrometers in size. Forsterite is very rare; only one prismatic crystal was detected during the electron microprobe work. It can be distinguished optically from pertsevite and clinohumite only with difficulty by its somewhat higher refraction, while birefringence is very similar. Like clinohumite, forsterite is also partially replaced by pertsevite. Ludwigite and the new alumino-magnesiohulsite occur in partly opaque aggregates consisting solely of these two minerals, which may have formed at the expense of an earlier high-temperature mineral (Pertsev *et al.*, submitted). The overall fabric of the rock, in which calcite is by far the dominant mineral, does not exhibit preferred orientation nor any other features indicating deformation.

Chemistry of pertsevite

Electron microprobe analyses were performed with the aid of the CAMECA SX 50 instrument at the Ruhr-Universität Bochum. The standards and lines used for the minerals studied in the present paper (pertsevite, clinohumite, forsterite, kotoite and spinel) were: synthetic pyrope (Si K_α, Al K_α, Mg K_α); synthetic andradite (Ca K_α, Fe K_α); synthetic spessartine (Mn K_α); synthetic TiO_2 (Ti K_α); synthetic Cr_2O_3 (Cr K_α); synthetic V_2O_3 (V K_α); natural topaz (F K_α); borosilicate glass (B K_α). As the optimal excitation conditions for boron differ from standard conditions for geological materials, the analyses of pertsevite, clinohumite and forsterite were made in two steps. First, the elements Si, Al, Mg, F, Ca, Mn and Fe were measured with a focused beam using 15 kV accelerating voltage and 15 nA beam current. Boron oxide was taken provisionally as the difference of the total to 100 %. In the second step the same sample spots were measured again, now excluding Fe and Mn from the above list but including boron, using 8 kV voltage and 100 nA current with a beam diameter of 10 micrometer. For boron, 100 s measuring time for peak and 50 s for each side of the background were used. The results for Si, Al, Mg, F, and Ca of the two measuring cycles were identical within the limits of error. Boron was measured using the CAMECA PC2 multilayer pseudocrystal for diffraction. The borosilicate glass mentioned above served as standard in order to avoid, or at least reduce, possible crystallographic orientation effects on peak shape or peak position for the standard (Bastin & Heijligers, 1986, 1990). There was no measurable peak shift between this standard and pertsevite. The area/peak factors of both, standard and pertsevite, were determined. Because they were found to be significantly different – probably owing to the different structures – a correction factor of 0.8 was calculated and applied to the boron values after processing with the PAP correction procedure (Pouchou & Pichoir, 1984).

An important result of the first microprobe investigations on pertsevite was its typically low, but always present and highly variable content of Si, even within single grains (Fig. 2). After boron could be analyzed as well, it became clear that there is a negative 1 : 1 correlation between the two elements (Fig. 4). This suggested that B and Si should essentially share common crystallographic sites in the structure of the new mineral.

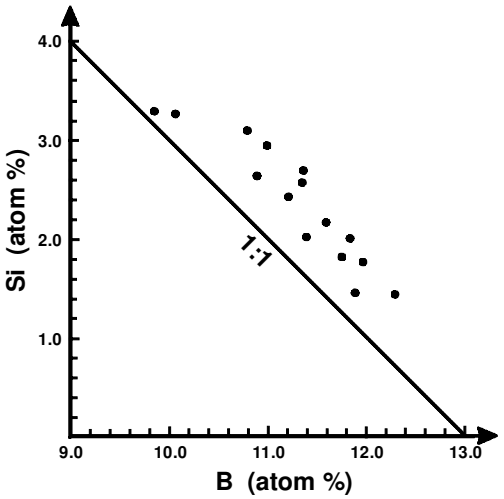

Fig. 4. Plot of atomic per cent concentrations of boron and silicon in 15 electron microprobe analyses taken in chemically heterogeneous crystals of pertsevite in thin section B-1048. The reference line indicates the quantitative relationship.

Because of the initially unknown anion contents of the new phase, in a first attempt only cation ratios were considered. In Fig. 5 the atomic percentages of 15 electron microprobe analyses for the elements (Mg+Fe+Mn), B and Si, normalized to 100, plot very close to a line connecting forsterite, Mg_2SiO_4, and a hypothetical phase "boroforsterite". This would have a formula "$Mg_2BO_{3.5}$" exhibiting an oxygen deficiency relative to forsterite. At any rate, the location of the analyses in Fig. 5 excludes the initial suspicion that the new silicate-borate mineral could be a highly boron-bearing derivative of the humite group.

In Table 1, a selection of ten pertsevite analyses is listed which cover a range of SiO_2 contents from about 4 to 12 wt.%. They are arranged in the order of increasing SiO_2. In addition to the major components MgO and B_2O_3, there is generally little Fe taken as FeO, as well as minor amounts of Mn, Ca and Al. No other elements with atomic numbers greater than six were detected. Interestingly, the crystals lowest in SiO_2 have the highest Fe, in one case also the highest Al. Among the anions fluorine is invariably present and probably also some hydroxyl.

Structural formulae were first calculated with the cation : anion ratio 3 : 4 of forsterite, Mg_2SiO_4, in mind. The absence of anion vacancies was subsequently confirmed by crystal structure analysis. The 3 : 4 ratio is equally applicable to a silicon-bearing phase related to $Mg_2(BO_3)F$. The introduction of Si into such pure borate was considered to be accompanied by partial replacement of fluorine by oxygen according to $Si^{4+} + O^{2-}$ for $B^{3+} + F^{1-}$. If this were so exclusively, the numbers of B p.f.u. and F p.f.u. should be equal. However, Table 1 shows that B is consistently larger than F p.f.u. Therefore, additional hydroxyl groups were calculated for charge balance, which requires H_2O amounts of about 1.6 to 2.3 wt.% among the oxides, but still keeps the oxide totals below 100 % (Table 1). The basic assumption of the formulae of Table 1 is that the total amount of cations (without hydrogen) is 3.00. The results obtained here by iteration show that the overall anion totals (= total 3 of Table 1) come very close to the ideal 4.00, while the cation totals 1 and 2 deviate more strongly from the ideal values 1.00 and 2.00, respectively. Considering analytical errors, especially for boron, this is quite acceptable. The assumption of hydroxyl in pertsevite is supported by the experience of Grigoriev & Brovkin (1969) that, in their hydrothermally synthesized α-$Mg_2(BO_3)F$ products, fluorine is also partially replaced by OH. Most importantly, an infrared microscope spectroscopic study by K. Röller, Bochum (personal communication 2002), on a persevite grain within our thin section B-1048

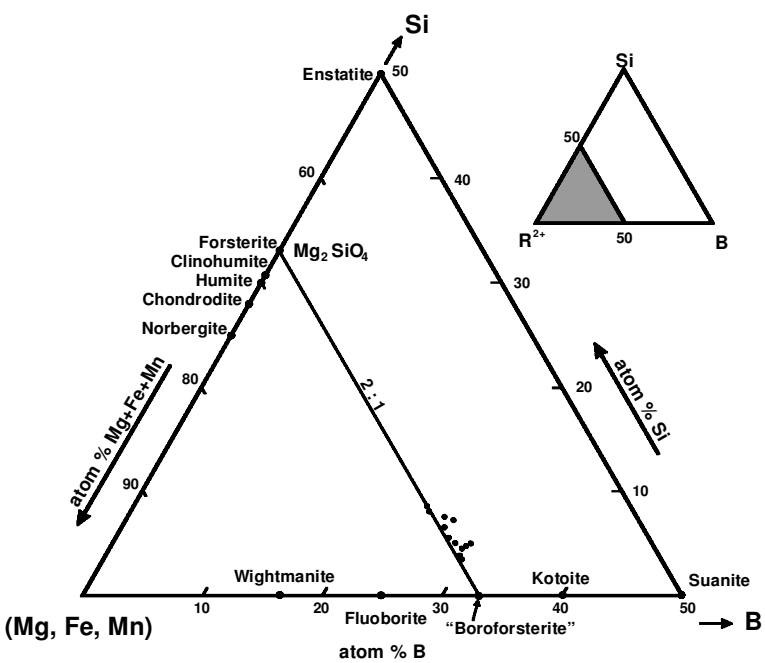

Fig. 5. Ternary plot of atomic percentages of (Mg + Fe + Mn), B, and Si of the pertsevite electron microprobe analyses performed on thin section B-1048. Only the Si- and B-poor portion with relevant minerals is shown in detail. Note that the data points plot close to a join extending from forsterite, Mg_2SiO_4, to a hypothetical phase "boroforsterite" with a potential formula "$Mg_2BO_{3.5}$". Line labelled 2:1 defines the constant cation ratio Mg : (B + Si).

Table 1. Electron microprobe analyses of pertsevite from sample B-1048.

No.:	43[2]	38	26	29	24	35[3]	1	17[4]	48[5]	45[5]	Range
SiO_2	4.37	4.85	5.32	6.23	7.03	8.25	8.75	9.86	10.28	11.66	4.37 – 11.66
B_2O_3	24.12	23.68	23.83	24.33	24.27	22.44	21.17	21.92	19.52	18.72	18.72 – 24.33
MgO	49.63	56.92	59.39	58.31	59.00	57.39	58.17	58.32	57.68	57.62	49.63 – 59.39
FeO	8.48	4.01	2.13	2.14	2.09	3.71	2.48	2.47	2.55	2.57	2.09 – 8.48
MnO	.44	.66	.35	.38	.36	.65	.44	.42	.43	.45	.35 – .66
CaO	.15	.26	.15	.10	.12	.24	.19	.12	.16	.09	.09 – .26
Al_2O_3	1.55	.14	.06	.06	.03	.10	.07	.04	.06	.07	.03 – 1.55
F	6.01	8.42	7.86	7.48	7.29	7.81	6.56	6.11	5.97	6.95	5.97 – 8.42
Total	94.75	98.94	99.09	99.03	100.19	100.59	97.83	99.26	96.65	98.13	
-O≡F	2.53	3.55	3.31	3.15	3.07	3.29	2.76	2.57	2.51	2.93	2.51 – 3.55
H_2O[1]	2.29	1.93	2.25	2.04	2.06	1.67	2.28	2.19	2.31	1.62	1.62 – 2.31
Total	94.51	97.32	98.03	97.62	99.18	98.97	97.35	98.88	96.44	96.82	

Number of ions per formula unit (for calculation see text)

No.:	43[2]	38	26	29	24	35[3]	1	17[4]	48[5]	45[5]	Range
Si	.101	.108	.116	.136	.152	.181	.195	.216	.232	.264	.101 – .264
B	.965	.909	.900	.917	.904	.851	.814	.827	.762	.731	.731 – .965
Total 1	1.066	1.017	1.016	1.053	1.056	1.032	1.009	1.043	.994	.995	
Mg	1.715	1.886	1.934	1.897	1.897	1.879	1.931	1.900	1.944	1.943	1.715 – 1.944
Fe	.164	.075	.039	.039	.038	.068	.046	.045	.048	.049	.038 – .164
Mn	.009	.012	.006	.007	.007	.012	.008	.008	.008	.009	.007 – .012
Ca	.004	.006	.003	.002	.003	.006	.004	.003	.004	.002	.002 – .006
Al	.042	.004	.001	.001	.001	.003	.002	.001	.002	.002	.001 – .042
Total 2	1.934	1.983	1.983	1.946	1.946	1.968	1.991	1.957	2.006	2 005	
F	.440	.592	.543	.516	.497	.543	.462	.422	.427	.497	.422 – .592
OH[1]	.354	.286	.328	.297	.297	.245	.339	.319	.348	.244	.244 – .354
O	3.208	3.125	3.131	3.188	3.207	3.214	3.202	3.259	3.227	3.259	3.125 – 3.259
Total 3	4.002	4.003	4.002	4.001	4.001	4.002	4.003	4.000	4.002	4.000	

No.: = original number of analysis. Footnotes: [1] calculated (see text); [2] coexisting with ludwigite; [3] used for structural and optical measurements; [4] coexisting with clinohumite; [5] coexisting with forsterite.

yielded unequivocal qualitative evidence for the presence of hydroxyl groups, a characteristic band at 3560 cm^{-1}.

In summary, the recalculations of Table 1 indicate that the ten pertsevite crystals analyzed here belong to a series of solid solution which leads from an ideal borate, $Mg_2BO_3(F,OH)$, eventually to a pure silicate, Mg_2SiO_4. The occurrence of virtually pure forsterite in the thin section B-1048 studied (see later) suggests that a large miscibility gap exists in this chemical system. Interestingly, the most silicatian pertsevite crystals analyzed (Table 1, Nos. 48 and 45) are those replacing, and thus coexisting with forsterite. On the other hand, the least silicatian pertsevite (No. 43 of Table 1) was found to lie directly adjacent to an aggregate of ludwigite as in Fig. 2, which may also explain its relatively high contents in Fe and Al (see also Pertsev *et al*., submitted).

Single-crystal X-ray diffraction

For the structural work, a crystal fragment, about 0.02 × 0.04 × 0.06 mm^3 in size, was separated from the thin section as part of a larger, rather homogeneous pertsevite crystal. Analysis No. 35 of Table 1 had been taken previously from a spot located on this fragment. Its composition lies about in the center of the range of pertsevite solid solution as shown in Fig. 4 and 5. The fragment was measured on a Siemens three-circle diffractometer (equipped with a CCD 1000K area detector and a flat graphite monochromator) using MoK_α X-radiation from a fine focus sealed tube (Table 2). The small crystal size required an exposure time of 6 min. per frame. A SMART system of programs (Bruker AXS, 1998) was used for cell dimension determination and X-ray data collection and SAINT+ (Bruker AXS, 1999) for the data reduction including intensity integration, background and Lorentz-polarization corrections. The program XPREP (Bruker AXS 1997) was used for empirical absorption correction based on pseudo Ψ-scans. The space groups $Pna2_1$ (acentric) and *Pnma* (centrosymmetric), proposed by the program XPREP (Bruker AXS, 1997), were both chosen for structure solution and refinement. Already after determination of the cell dimensions (a = 20.490(6), b = 4.571(1), c = 11.890(3) Å), it became evident that pertsevite is closely related to synthetic α-Mg_2BO_3F (Brovkin & Nikishova, 1975) with slightly smaller cell dimensions (a = 20.44(2), b = 4.530(5), c = 11.80(1) Å). Nevertheless, the structure was solved by direct methods (program SHELXS by Sheldrick,

Table 2. Parameters for X-ray data collection and crystal structure refinement of pertsevite.

Diffractometer	Siemens Smart CCD
X-ray radiation	MoK_α (0.71073 Å)
X-ray power	50 kV, 40 mA
Temperature	293 K
Crystal size (mm)	0.02 × 0.04 × 0.06
Detector to sample distance	5.2 cm
Rotation axis	ω
Rotation width	0.3°
Total number of frames	1271
Frame size	512 × 512 pixels
Time per frame	360 sec
Space group	$Pna2_1$ (Nr. 33)
Cell dimensions (Å)	a=20.490(6), b=4.571(1), c=11.890(3)
Z	16
Collection mode	Automated hemisphere
Reflections collected	6492
Max. 2 θ	56.5
Index range	-26 ≤ h ≤ 26 -2 ≤ k ≤ 6 -14 ≤ l ≤ 15
Unique reflections	2416
Reflections > 2σ(I)	1330
R_{int}	0.066
R_σ	0.079
Number of least squares parameters	106
GooF	1.228
$R1$, I > 2σ(I)	0.064
$R1$, all data	0.136
W$R2$ (on F^2)	0.150

Table 3. Atomic coordinates and isotropic displacement parameters for pertsevite.

Atom	Occupancy	X/a	y/b	z/c	B (Å^2)
Mg1	1.0	0.3780(1)	0.5195(7)	0.2506(8)	0.75(2)
Mg2	1.0	0.6179(1)	0.9879(8)	0.2455(5)	0.75(2)
Mg3	1.0	0.2464(3)	0.532(1)	0.1137(5)	0.75(2)
Mg4	1.0	0.2479(3)	0.532(1)	0.3903(4)	0.75(2)
Mg5	1.0	0.3784(3)	0.517(1)	-0.0205(4)	0.75(2)
Mg6	1.0	0.3768(4)	0.519(2)	0.5256(4)	0.75(2)
Mg7	1.0	0.4850(3)	0.995(1)	0.1234(4)	0.75(2)
Mg8	1.0	0.5117(3)	0.978(1)	-0.1227(4)	0.75(2)
O1	1.0	0.3339(6)	0.766(3)	0.1148(9)	0.96(3)
O2	1.0	0.3375(6)	0.769(3)	0.390(1)	0.96(3)
O3	1.0	0.2033(3)	0.769(1)	0.256(1)	0.96(3)
O4	1.0	0.3286(6)	0.713(3)	-0.1505(8)	0.96(3)
O5	1.0	0.1705(7)	0.238(3)	0.1471(8)	0.96(3)
O6/F	1.0	0.4619(7)	0.750(4)	-0.0068(9)	0.96(3)
O7/F	1.0	0.5368(7)	0.249(4)	0.0082(9)	0.96(3)
O8/F	1.0	0.5308(3)	0.244(1)	0.245(1)	0.96(3)
O9	1.0	0.4013(6)	0.213(3)	0.1200(9)	0.96(3)
O10	1.0	0.3992(6)	0.219(3)	0.3856(8)	0.96(3)
O11	1.0	0.1992(7)	0.719(3)	-0.013(1)	0.96(3)
O12	1.0	0.3018(7)	0.211(3)	0.0189(9)	0.96(3)
O13/F	1.0	0.4663(3)	0.702(1)	0.250(1)	0.96(3)
O14/F	1.0	0.4239(4)	0.243(2)	-0.1228(6)	0.96(3)
O15	1.0	0.5675(4)	0.705(2)	0.1505(6)	0.96(3)
O16/F	1.0	0.2884(3)	0.317(1)	0.250(1)	0.96(3)
B1	0.91(1)	0.3435(9)	0.044(4)	0.418(1)	0.36(9)
Si1	0.09(1)	0.330(2)	0.117(8)	0.372(3)	0.36(9)
B2	0.60(5)	0.523(1)	0.530(6)	0.220(2)	0.36(9)
B2A	0.15(3)	0.522(3)	0.58(1)	0.034(5)	0.36(9)
Si2	0.25(1)	0.5346(6)	0.576(3)	0.263(2)	0.36(9)
B3	0.73(1)	0.1848(8)	0.067(3)	0.243(2)	0.36(9)
Si3	0.27(1)	0.2103(5)	0.108(2)	0.258(2)	0.36(9)
B4	1.0	0.3450(9)	0.079(4)	0.093(1)	0.36(9)

1997a) that revealed about ¾ of the atom positions. In subsequent refinement cycles (program SHELXL by Sheldrick, 1997b), applying scattering factors for neutal atoms, additional atomic positions were deduced from the difference Fourier syntheses. Comparison between $Pna2_1$ (acentric) and *Pnma* (centrosymmetric) refinements indicated the acentric model to be correct (additional details are discussed below) and also to be in agreement with the structure of synthetic α-Mg_2BO_3F (Brovkin & Nikishova, 1975). Due to correlations imposed by the pseudo-centric structure, isotropic displacement parameters were refined. In addition, to minimize the number of variables, atomic sites occupied by the same species were refined with the same displacement parameters. Occupancy constraints were set up to model the partial occupation of tetrahedral voids. It was assumed that either a triangular tetrahedral face is occupied by B, or that Si resides in the center of the tetrahedron. Atomic coordinates are given in Table 3 and interatomic distances are summarized in Table 4. The atomic coordinates and occupancies (Table 3) were used to calculate an X-ray powder pattern (otherwise not available) for CuK_α X-radiation and diffractometer (Debye-Scherrer) geometry (Table 5) using the program LAZYPULVERIX (Yvon *et al.*, 1977).

Structure description

Pertsevite, although with a stoichiometry similar to olivine, has a topologically different structure. The common features of both structures are hexagonal closest anion (O, OH, F) packing with 50 % of the octahedral voids occupied by Mg. The characteristic Mg arrangement in the new mineral derived from α-Mg_2BO_3F (Brovkin & Nikishova, 1975) can be described by edge-sharing chains of Mg7 and Mg8 octahedra running parallel to c (Fig. 6). Triangular units of clusters formed by six edge-sharing octahedra (M1-M6), oriented parallel to (010), are alternately attached to both sides of the straight octahedral chains (Mg7, Mg8). Adjacent (010) layers are symmetrically related to the central layer in a way that the octahedral voids in the central layer are occupied in the adjacent layer and *vice versa* (Fig. 6). Triangular BO_3 units in α-Mg_2BO_3F (Brovkin & Nikishova, 1975) were located on selected tetrahedral faces of tetrahedral vacancies characteristic of closest packed structures. In pertsevite several boron sites are only partly filled and instead the tetrahedral vacancies are occupied by Si where charge balance is obtained according to $Si^{4+} + O^{2-} \leftrightarrow B^{3+} + (F,OH)^-$. The ar-

Table 4. Selected interatomic distances for pertsevite.

Mg1 -	O13	1.993(6)	Mg5 -	O14	1.978(10)
	O16	2.055(6)		O6	2.022(16)
	O9	2.145(13)		O4	2.057(13)
	O10	2.158(13)		O12	2.152(16)
	O1	2.165(14)		O1	2.170(13)
	O2	2.173(14)		O9	2.221(13)
Average		2.114	Average		2.100
Mg2 -	O15	2.002(9)	Mg6 -	O5	2.007(13)
	O5	2.032(13)		O7	2.073(17)
	O14	2.073(9)		O11	2.127(16)
	O3	2.112(7)		O15	2.134(10)
	O8	2.136(6)		O2	2.138(13)
	O4	2.143(12)		O10	2.204(13)
Average		2.083	Average		2.114
Mg3 -	O11	1.987(14)	Mg7 -	O6	1.969(15)
	O16	2.079(15)		O9	1.983(15)
	O1	2.088(14)		O13	2.054(13)
	O5	2.092(14)		O8	2.063(10)
	O12	2.168(14)		O7	2.085(15)
	O3	2.193(12)		O15	2.172(11)
Average		2.101	Average		2.054
Mg4 -	O12	2.010(13)	Mg8 -	O6	2.007(15)
	O16	2.108(15)		O10	2.037(15)
	O11	2.129(14)		O7	2.054(14)
	O2	2.131(15)		O8	2.068(11)
	O3	2.135(13)		O13	2.148(13)
	O4	2.195(14)		O14	2.169(11)
Average		2.118	Average		2.081
B1 -	O1	1.31(2)	B3 -	O5	1.41(2)
	O11	1.44(2)		O3	1.42(1)
	O10	1.44(2)		O4	1.46(2)
B2 -	O8	1.35(2)	B4 -	O9	1.35(2)
	O13	1.45(2)		O12	1.39(2)
	O15	1.47(2)		O1	1.47(2)
B2A -	O6	1.54(7)			
	O7	1.57(7)			
	O15	1.76(6)			
Si1 -	O10	1.49(4)	Si3 -	O4	1.436(18)
	O11	1.56(3)		O3	1.550(10)
	O2	1.61(4)		O5	1.656(19)
	O16	1.92(4)		O16	1.865(12)
Si2 -	O13	1.522(13)			
	O8	1.530(15)			
	O15	1.606(17)			
	O14	1.81(2)			

rangement of BO_3 units and SiO_4 tetrahedra in this structure is shown in Fig. 7.

Forsterite, Mg_2SiO_4, with Z = 4 has a unit-cell volume of 290 Å^3, whereas Mg_2BO_3F with Z = 16 has a cell volume of 1092.6 Å^3 (Brovkin & Nikishova, 1975) indicating that the packing in α-Mg_2BO_3F (1092.6/4 = 273 Å^3) is more compact than in forsterite. The pertsevite crystal investigated by us had *ca.* 15 % B replaced by Si leading to a volume of 1113.6 Å^3. Allowing $O^{2-} \rightarrow (F, OH)^-$ substitution for charge balance, the refined formula is $Mg_2(BO_3)_{0.85}(SiO_4)_{0.15}(F, OH)_{0.85}$, which is close to analysis No. 35 of Table 1. Minor Fe replacing Mg could not be located.

Table 5. X-ray powder pattern of pertsevite (calculated from coordinates obtained by single-crystal structure refinement) for CuK_α radiation and diffractometer (Debye-Scherrer) geometry, space group $Pna2_1$, $a = 20.490$, $b = 4.571$, $c = 11.890$ Å. The 10 strongest lines are underlined.

I/I$_0$	d (Å)	h	k	l
2	7.7613	2	0	1
4	5.9450	0	0	2
15	5.1420	2	0	2
18	4.1770	1	1	1
5	3.9387	2	1	1
3	3.8806	4	0	2
24	3.7988	3	1	0
15	3.6964	2	0	3
4	3.6186	3	1	1
6	3.4150	6	0	0
6	3.2823	6	0	1
1	3.2784	4	1	1
2	3.2011	3	1	2
5	3.1346	4	0	3
15	3.0513	5	1	0
5	2.9630	1	1	3
5	2.9583	4	1	2
2	2.8742	2	1	3
1	2.8548	2	0	4
77	2.7425	3	1	3
32	2.7146	5	1	2
2	2.6661	6	1	1
2	2.5871	6	0	3
2	2.5852	4	1	3
5	2.5710	4	0	4
6	2.5612	8	0	0
49	2.4737	1	1	4
32	2.4178	5	1	3
46	2.4137	7	1	1
5	2.2770	7	1	2
6	2.2714	1	2	0
100	2.2409	4	1	4
49	2.2344	8	1	0
2	2.2311	1	2	1
2	2.1569	4	0	5
2	2.1512	8	0	3
3	2.1322	3	2	1
3	2.1292	5	1	4
1	2.1218	1	2	2
1	2.0192	10	0	1
5	2.0156	3	1	5
2	2.0086	9	1	1
3	1.9817	0	0	6
2	1.9507	4	1	5
2	1.9439	2	2	3
3	1.9278	9	1	2
1	1.9016	3	2	3
1	1.8994	6	2	0
8	1.8975	7	1	4
2	1.8756	6	2	1
3	1.8470	10	1	1
2	1.8467	4	2	3
1	1.7948	6	1	5
3	1.7250	11	1	0
3	1.7128	6	2	3
92	1.7081	4	2	4
44	1.7053	8	2	0
2	1.6910	10	1	3
2	1.6880	8	2	1
3	1.6870	10	0	4
7	1.6808	9	1	4
5	1.6757	2	0	7
2	1.6619	5	1	6
3	1.6269	2	2	5
1	1.5922	0	1	7
9	1.5874	1	1	7
3	1.5827	10	1	4
12	1.5817	11	1	3
3	1.5682	12	0	3
2	1.5673	8	0	6
2	1.5664	8	2	3
4	1.5523	10	0	5
1	1.5445	7	1	6
2	1.5208	6	0	7
3	1.5072	1	3	1
2	1.4972	0	2	6
3	1.4901	13	1	0
3	1.4871	3	3	0
21	1.4863	0	0	8
41	1.4806	12	0	4
1	1.4721	1	3	2
2	1.4636	14	0	0
2	1.4427	3	3	2
3	1.4281	5	3	0
1	1.4156	8	0	7
2	1.4087	2	3	3
13	1.3987	7	1	7
1	1.3963	11	1	5
4	1.3923	3	3	3
2	1.3870	12	0	5
2	1.3841	3	1	8
1	1.3730	14	0	3
1	1.3704	4	3	3
2	1.3530	1	3	4
3	1.3436	5	3	3
4	1.3429	7	3	1
1	1.3129	6	3	3
10	1.3108	4	3	4
1	1.3103	2	0	9
6	1.3095	8	3	0
2	1.3048	9	1	7
1	1.3016	8	3	1
5	1.3009	15	1	1
1	1.2855	8	0	8
1	1.2730	2	3	5
5	1.2375	8	1	8
2	1.2303	7	3	4
1	1.1437	17	1	2
6	1.1428	0	4	0
1	1.1325	1	3	7
3	1.1304	11	3	3
8	1.1204	8	2	8
4	1.1172	16	2	0
1	1.1123	16	2	1

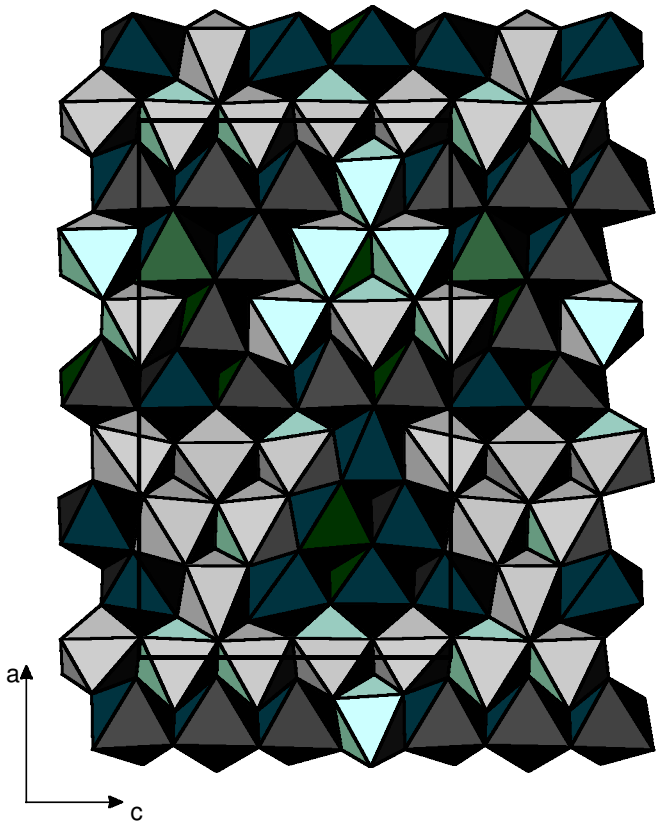

Fig. 6. Arrangement of MgO_6 octahedra in the structure type of α-$Mg_2(BO_3)F$ (Brovkin & Nikishova, 1975) and of pertsevite. Octahedra of the upper (010) layer are light grey and those of the lower layer are dark grey. Octahedral voids in the upper layer are occupied in the adjacent layer and *vice versa*. Labels for Mg octahedra are displayed in Fig. 7.

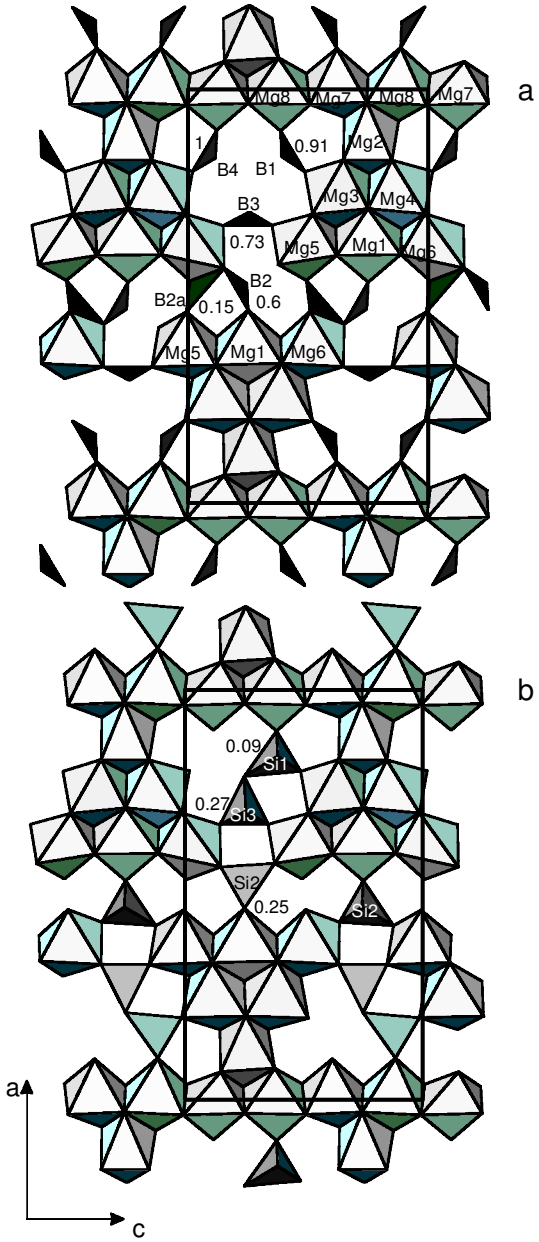

Fig. 7a. Arrangement of BO_3 triangles in the refined structure of $Mg_2(BO_3)_{0.85}(SiO_4)_{0.15}(OH,F)_{0.85}$. Numbers close to the B1-B4 labels represent boron occupancies. 7b. Arrangement of SiO_4 tetrahedra in the refined structure of $Mg_2(BO_3)_{0.85}(SiO_4)_{0.15}(OH,F)_{0.85}$. Numbers close to the Si1, Si2, Si3 labels represent silicon occupancies.

The major reason why a compound Mg_2SiO_4 with the structure type of α-Mg_2BO_3F cannot exist is the occurrence of three SiO_4 tetrahedra bonded to one common O site (O16) also participating in three Mg octahedra. This oxygen (O16) can for bond-strength reasons only accept additional bonding to one SiO_4 tetrahedron. Thus, for crystal chemical reasons, only B2 and either B4, B3, or B1 can be completely substituted by Si leading to an end-member formula of $Mg_2(SiO_4)_{0.5}(BO_3)_{0.5}(F,OH)_{0.5}$ for the theoretically most silicatian variety of pertsevite.

The pertsevite structure has a pseudo-mirror plane perpendicular to the c-axis (at z = ¼) resulting from the distribution of the MgO_6 octahedra. However, the distribution of the B positions B2 and B2A does not agree with this mirror plane. In addition, the edges of the BO_3 triangles formed by O13-O15, O15-O8, O8-O13 are 2.39, 2.50, and 2.47 Å long, whereas the corresponding distances of a hypothetical mirror plane related site B2' are 2.97 Å (O8-O14) and 2.72 Å (O14-O13) with O8-O13 common to both triangles. This clearly indicates that also the distortion of some MgO_6 octahedra is not in agreement with the mirror plane perpendicular to *c*. It is for this reason that the structure is definitely acentric (space group $Pna2_1$) and not centrosymmetric *Pnma* (with *b* and *c* interchanged in standard setting). Nevertheless we have tested *Pnma* refinements and found particularly poor agreement between observed and calculated structure factors of low intensity reflections. In addition, the *Pnma* refinement required several split oxygen positions. The original structural study on synthetic α-Mg_2BO_3F was also performed in $Pna2_1$ symmetry but the question arose whether acentricity is still maintained for a partially SiO_4 substituted mineral. A fully SiO_4 substituted variety of this mineral, $Mg_2(SiO_4)_{0.5}(BO_3)_{0.5}(F, OH)_{0.5}$, would probably be centrosymmetric (*Pnma*) because Si replacing B2 is located on the mirror plane and, as discussed above, B1, B3, and B4 can only statistically be replaced by Si. The highly signifi-

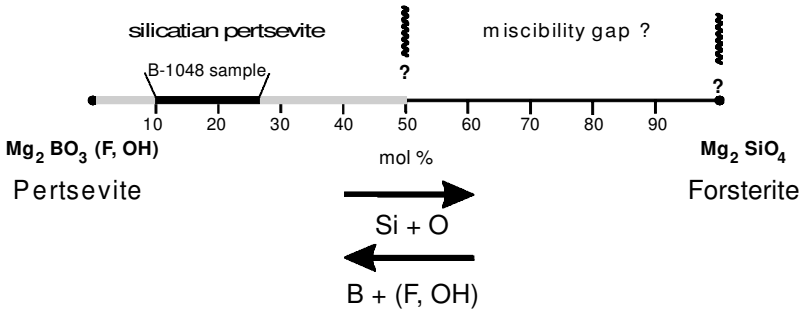

Fig. 8. Join of binary solid solution between pertsevite and forsterite end members. The underlying ionic substitutions are indicated at the bottom. Note the analyzed range of pertsevite compositions in thin section B-1048 (heavy black bar). We propose to use the name *silicatian pertsevite* for the range up to 50 mol% forsterite. For the miscibility gap a minimum width is shown based on analytical data of forsterite from sample B-1048 (Table 6) and structural considerations for pertsevite (see text).

cant but nevertheless slight deviation of the mineral structure from centrosymmetry causes strong correlations among positions related by pseudosymmetry. For this reason, the esd's of coordinates are fairly high. In addition, the refined pertsevite structure is disordered due to the partial $SiO_4 \rightarrow (BO_3)(F, OH)$ substitution (27 % at maximum for an individual site, *e.g.* Si3) and as a consequence of this the tetrahedral SiO_4 geometry strongly deviates from ideal. Because of the low quality of the data (small crystal), expected smearing of oxygen/fluorine sites due to disorder could not be resolved. All anion sites (O, OH, F) not bonded to B are mixed O, (F,OH) sites (O14/F and O16/F) depending on the Si substitution. Furthermore, due to the disordered occupancy of B2 and B2A, the anion sites O6/F, O7/F, O8/F, and O13/F have a mixed F,O occupancy.

Definitions

Following the rules of defining and naming new minerals (Nickel & Mandarino, 1987; Nickel & Grice, 1998) it is clear that the name pertsevite must be applied to the end member of the solid solution series described here, that is to the pure borate-fluoride phase Mg_2BO_3F, although this has not been detected in the sample available. This implies that one particularly interesting structural feature of these new mineral phases, that is the partial replacement of boron in triangular coordination by silicon with concomitant enlargement of the coordination sphere from three to four, is not part of this end-member definition. Thus, these phases must be defined by an adjectival modifier, and we suggest to name them *silicatian pertsevites* as members of the series of solid solutions toward forsterite (Fig. 8). A general formula of silicatian pertsevite may be given as $Mg_2(B,Si)O_3(F,OH,O)$. Table 1 shows that in all our silicatian pertsevites anlyzed here, fluorine predominates over OH. Therefore, also with respect to these two components, the end-member formula defined for pertsevite above is correct. However, it may be expected that hydroxyl-dominant pertsevite exists as well. As outlined previously, the compositional extent of silicatian pertsevites should, for structural reasons, not exceed the theoretical end member $Mg_2(BO_3)_{0.5}(SiO_4)_{0.5}(F,OH)_{0.5}$ or $Mg_2(B_{0.5}\ Si_{0.5}O_{3.5})(F,OH)_{0.5}$. Thus the miscibility gap in the system should have a minimum width from 50 to practically 100 mol% Mg_2SiO_4 (Fig.8). A general formula for pertsevite showing these compositional restrictions would be $Mg_2(BO_3)_{0.5+x}(SiO_4)_{0.5-x}(F,OH)_{0.5+x}$, with x ranging from 0 to 0.5. According to Table 1 and Fig. 5, x ranges in sample B-1048 from about 0.10 to 0.26 (Fig. 8). Therefore, under the conditions of crystallization of this contact rock, the miscibility gap between forsterite and silicatian pertsevite is much wider than the theoretically possible one.

Remaining physical properties of silicatian pertsevite

Because of the small sample size (one thin section), clear observations or even measurements of crystal properties of silicatian pertsevite are difficult or impossible. No characteristic crystal morphology was found, the grains always being anhedral with diameters up to 150 micrometers. In thin section, silicatian pertsevite is transparent and colorless. No cleavage, parting and twinning was observed. Fractures are uneven. Fluorescence and hardness could not be determined. Silicatian pertsevite is not cathodoluminescent under the electron beam.

Optically, silicatian pertsevite is biaxial positive. The refractive indices (for 589 nm) of the crystal studied by single-crystal methods (Table 1, No. 35) are: $\alpha = 1.609(1)$, $\beta = 1.620(1)$, $\gamma = 1.642(1)$ leading to a birefringence of 0.033, which is very similar as for both clinohumite and forsterite. $2V_Z$ could be measured as 65(1)°; the calculated value is 71(6)°. There is no dispersion of 2V visible. The density calculated for the crystal of analysis No. 35 (Table 1) is 3.12 g/cm^3. The compatibility index (Mandarino, 1979) was calculated to be –0.033, which places this silicatian pertsevite into the category "Excellent". Note that refraction and, especially, birefringence vary with the B/Si ratio of silicatian pertsevite. No reliable measurements could be made, however, in the often very heterogeneous grains (*e.g.*, Fig. 2). Qualitatively, it is clear from our thin section that birefingence increases with increasing boron contents. For the synthetic end member Mg_2BO_3F, Grigoriev & Brovkin (1969) report a birfringence of 0.037 with $\alpha = 1,571$ and $\gamma = 1.608$.

Chemistry of coexisting minerals

In the present paper, only analyses of the highly Mg-rich minerals of thin section B-1048 are reported. For the iron-

Table 6. Electron microprobe analyses of minerals coexisting with pertsevite (sample B-1048).

	Clinohumite			Forste-rite	Kotoite		Spinel
No.:	2	7	18	49	—	—	—
SiO_2	35.48	34.57	35.31	41.46	.31	.23	——
Al_2O_3	.02	.02	.03	.02	.00	.00	70.95
B_2O_3	1.31	1.57	1.40	.00	36.83[2]	36.08[2]	——
MgO	55.18	55.18	55.62	54.95	62.01	59.68	27.02
FeO	1.64	1.74	1.91	.92	.68	3.37	.89
MnO	.24	.26	.34	.05	.08	.45	——
CaO	.03	.07	.08	.02	.07	.18	——
F	2.91	3.17	4.00	.00	——	——	——
Total	96.81	96.58	98.69	97.42	99.98	99.99	99.36
-O≡F	1.23	1.33	1.68	——	——	——	——
H_2O[1]	1.67	1.71	1.31	——	——	——	——
Total	97.25	96.96	98.32	97.21	99.98	99.99	99.36[3]
Number of ions per formula unit							
On the basis of	18 (O, OH, F)	18 (O, OH, F)	18 (O, OH, F)	4 oxy-gens	6 oxy-gens	6 oxy-gens	4 oxy-gens
Si	3.792	3.705	3.742	1.001	.010	.007	——
B	.242	.290	.256	——-	2.017	2.007	——
Total 1	4.034	3.995	3.998	1.001	2.027	2.014	——
Al	.002	.002	.004	0.001	.000	.000	2.000
Mg	8.791	8.814	8.785	1.978	2.933	2.867	.963
Fe^{2+}	.147	.156	.169	0.019	.018	.091	.018
Mn	.022	.024	.030	0.001	.002	.012	——
Ca	.003	.008	.009	0.001	.002	.006	——
Total 2	8.965	9.004	8.997	2.000	2.955	2.976	2.992[4]
OH[1]	1.187	1.223	.926	——	——	——	——
F	.984	1.074	1.340	——	——	——	——
O	15.829	15.702	15.734	——	——	——	——

No. = original number of analysis, [1] calculated (see text), [2] calculated by difference, [3] includes TiO_2 0.25; V_2O_3 0.25; Cr_2O_3 0.04, [4] includes Ti 0.004; V 0.005: Cr 0.002

bearing borate mineral ludwigite and the new mineral alumino-magnesiohulsite the reader is referred to the companion paper by Pertsev *et al*. (submitted).

Clinohumite

In Table 6 the results of three electron microprobe analyses on portions of clinohumite crystals directly adjacent to pertsevite (*e.g.* Fig. 1 and 3) are listed. Interestingly, this clinohumite invariably contains appreciable amounts of boron as well. The formulae calculated imply that boron substitutes for silicon in the tetrahedral sites where it makes up between 6 and 7 mol%. B_2O_3 values are close to, or even exceed, the maximum boron contents of clinohumite, chondrodite and olivine as listed by Grew (1996, Table 17). The amount of OH was calculated for charge balance, maintaining 18 (O,OH,F). The octahedral element ratios M = Mg/(Mg+Fe+Mn) are generally slightly higher (0.98) than for persevite (0.90-0.98), so that there is actually a weak tendency for iron to fractionate into pertsevite relative to clinohumite. Note that, due to its textural position in the thin section next to pertsevite, the clinohumite crystal analyzed could be saturated in boron, if equilibrium was attained. Conversely, those portions of pertsevite close to clinohumite should be rich in Si. This holds for analysis No. 17 of Table 1 taken from a pertsevite protrusion within the large clinohumite crystal of Fig. 3.

Forsterite

Table 6 also lists the electron microprobe analysis taken from the one crystal of forsterite detected in section B-1048. Surprisingly, no boron and no fluorine could be found using the same analytical technique as for pertsevite and clinohumite, although forsterite is in direct contact with pertsevite. Perhaps forsterite was even depleted in boron by the replacing pertsevite under non-equilibrium conditions. The octahedral element ratio M (0.99) of forsterite is the highest of all the Mg-dominant phases.

Kotoite

The two electron microprobe analyses of kotoite reported in Table 6 give almost the ideal formula $Mg_3(BO_3)_2$, although boron was only calculated by difference in this case, and except that some Fe^{2+} and little Mn^{2+} substitute for Mg.

Spinel

The spinel phase (Table 6) is almost ideal end member $MgAl_2O_4$ with perfect stoichiometry and only trace amounts of Fe, Ti, V and Cr.

Petrology

Neglecting ludwigite and the new hulsite-group mineral (Pertsev *et al*., submitted), four phases of strongly Mg-dominated borates and silicates were found in sample B-1048: kotoite, silicatian pertsevite, clinohumite and forsterite. In the ternary projection of the oxide system of Fig. 9, which ignores Fe, Mn etc., these phases are plotted with their analyzed compositions and their compatibilities indicated. In the presence of the additional volatile components shown, all four phases could actually occur in mutual equilibrium. Nevertheless, with the limited experience on coexisting minerals in a single thin section only partly studied by EMP, there is direct evidence solely for the tie lines pertsevite-forsterite, pertsevite-clinohumite and pertsevite-kotoite. For these pairs we found the highest Si-contents of the silicatian persevite when coexisting with forsterite, relatively high values when in contact with clinohumite, and variable Si for pertsevite-kotoite (see schematic tie lines of Fig. 9 and footnotes 2, 4 and 5 in Table 1).

Uncertainty for a paragenetic discussion derives from the fact that silicatian pertsevite is a relatively late phase of the rock, clearly replacing clinohumite (Fig. 1) and forsterite. Could this suggest that there was a first (high-temperature?)

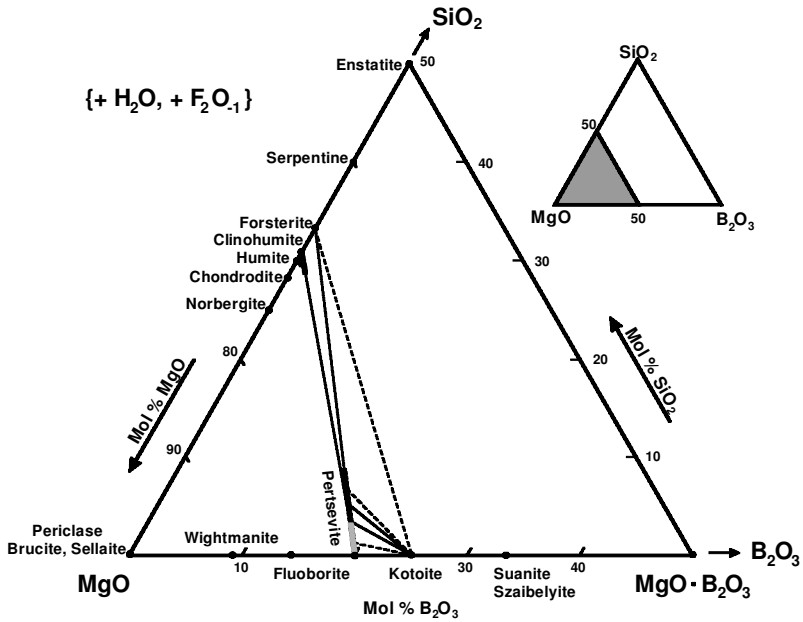

Fig. 9. Mg-rich portion of the ternary system MgO-B_2O_3-SiO_2 with excess water and fluorine showing relevant borate and silicate minerals. The new mineral pertsevite, ideally Mg_2BO_3F, forms silicatian solid solutions toward forsterite (Fig. 8), along which the solid bar characterizes the range of compositions analyzed in sample B-1048. Thin solid tie lines connect coexisting phases in this sample, dashed ones are inferred. Note boron solid solution in clinohumite as analyzed (Table 6).

assemblage forsterite + kotoite + clinohumite, and that clinohumite and kotoite reacted later with a hydrous, magnesian, fluorine-bearing fluid to form silicatian pertsevite? This would be supported by the lack of mutual contacts between kotoite and clinohumite in thin section B-1048. Another possibility for late pertsevite growth would be leaching out of B_2O_3 from the initial kotoite-clinohumite-forsterite rock by hydrous, F-bearing fluids.

No indications can be offered as to the conditions of formation of the silicatian pertsevite, except that it must have occurred prior to the secondary alteration of kotoite to szaibelyite and brucite during a very late hydrothermal phase. For Si-free pertsevite, temperatures below 750° C (Grigoriev & Brovkin, 1969) would have to be invoked, but there may be a stabilizing influence by the partial replacement of boron by silicon.

Because of the deceiving optical similarity of silicatian pertsevite with clinohumite and even forsterite, it seems possible that the new mineral has previously been overlooked, and that it is actually a more common, perhaps even a characteristic phase in Mg-boron-metasomatic skarns. According to N.N. Pertsev (personal communication 2002) there are strong indications for other occurrences. Extensive searches employing the electron microprobe are warranted.

Another challenge would be to find the Si-free end-member pertsevite, $Mg_2BO_3(F,OH)$, in nature, which could occur in assemblages with other Mg-borate minerals such as fluoborite, $Mg_3(BO_3)(F,OH)_3$, szaibelyite, $MgBO_2(OH)$, and wightmanite, $Mg_5O(BO_3)(OH)_5{\cdot}2H_2O$ (Fig. 9). Its appearance depends, of course, on its yet unknown pressure-temperature stability field. Grigoriev & Brovkin (1969) report on hydrothermal syntheses of this phase, with or without additional kotoite, fluoborite and szaibelyite, between 350 and 600° C, with higher yields at increasing temperatures. If it is a low-temperature phase as well, end-member pertsevite may even be found in low-grade metamorphic evaporite deposits.

Chemical and structural comparisons

For the system MgO-B_2O_3-SiO_2(-H_2O-F_2O_{-1}) projected in Fig. 9, the new mineral silicatian pertsevite represents a unique chemical and structural linkage between pure borates and pure silicates. Even when silicon of the silicates is partially replaced by boron such as in the humite-group minerals (Table 6 and Grew, 1996, Table 17), this takes place without a change of coordination against the anions. Mg-borates carrying (BO_3)-groups like kotoite contain only very minor amounts of silicon (Table 6 and Woodford *et al.*, 2001). In silicatian pertsevite, however, trigonally coordinated boron can be extensively and continuously replaced by tetrahedrally coordinated silicon, thus leading, at least theoretically, to a 1:1 intermediate borate-silicate (Fig. 8).

Among natural minerals, such "multi-coordination", gradual B/Si-exchange seems to be a very rare case, and this may also be true for synthetic products. Similar *chemical* relations may hold in the system Al_2O_3-B_2O_3-SiO_2 where, in fact, some pure Al-borates are essentially isostructural with the silicates sillimanite and/or mullite (Garsche *et al.*, 1991). They may indeed form extensive ranges of metastable(?) solid solutions toward the silicates, the "boron-mullites" (see Werding & Schreyer, 1996, sections 3.5. and 3.6.). The natural mineral boralsilite, $Al_{16}B_6Si_2O_{37}$ (Grew *et al.*, 1998), is a distinct intermediate phase between borates and silicates. However, its crystal structure built up of SiO_4-, BO_4- and BO_3-coordination polyhedra (Peacor *et al.*, 1999) does not show any indications of an "intrusion" of Si into BO_3-triangles as in pertsevite. Nevertheless, this could be a *structural* mechanism applying to the "boron-mullites", the disordered and perhaps metastable intermediate Al-borate-silicate solid solutions (see also Pöter *et al.*, 1998).

In the more complex system also involving Mg, the structural relationship of werdingite, $Mg_2Al_{14}B_4Si_4O_{37}$, to sillimanite is based on a partial replacement of $^{[4]}Si$ by $^{[3]}B$ (Niven *et al.*, 1991). Note, however, that in these cases the sub-

stitution is connected with a loss of anions and the appearance of structural vacancies (B + □ = Si + 0.5O; Werding & Schreyer, 1992). Only the involvement of fluorine (or OH) as in silicatian pertsevite allows the maintenance of a vacancy-free anion arrangement.

Acknowledgements: We thank Nick Pertsev for providing the thin section and for permission to extend the initially planned joint research program into the unknown. K. Röller, Bochum, ran infrared spectra of pertsevite grains in thin section B-1048 by microscope spectrometry thus confirming hydroxyl groups. Frau R. Lehmann at Bochum prepared the line drawings. E.S. Grew and J.D. Grice provided constructive journal reviews.

References

Aleksandrov, S.M., Troneva, M.A., Kurilchikova, G.E. (2000): Tin-bearing borates of hulsite-paigeite series from skarn deposits of Northeastern Russia: composition and geochemical evidence for genesis. *Geochemistry International*, **38,** 676-688.

Bastin, G.F. & Heijligers, H.J.M. (1986): "Quantitative electron probe microanalysis of boron in binary borides." Eindhoven, University of Technology, Publ. of the Lab. for Physical Chemistry, 115 p.

–, – (1990): Quantitative electron probe microanalysis of ultralight elements (boron – oxygen). *Scanning*, **12**, 225-236.

Brovkin, A.A. & Nikishova, L.V. (1975): The crystal structure of α-Mg_2BO_3F and the isomorphic substitution $(3F)^{3-} \leftrightarrow (BO_3)^{3-}$. *Sov. Phys. Crystallogr.*, **20**, 452-455.

Bruker AXS (1997): XPREP Ver. 5.1: A computer program for data preparation and reciprocal space exploration. Bruker Analytical X-ray systems, Madison, WI 53719-1173, USA.

Bruker AXS (1998): SMART Ver. 5.0/NT: A software package for CCD detector systems. Bruker Analytical X-ray systems, Madison, WI 53719-1173, USA.

Bruker AXS (1999): SAINT+ Ver. 6.01/NT: A computer program for data reduction. Bruker Analytical X-ray systems, Madison, WI 53719-1173, USA.

Garsche, M., Tillmanns, E., Almen, H., Schneider, H., Kupčik, V. (1991): Incorporation of chromium into aluminium borate 9 $Al_2O_3 \cdot 2B_2O_3$ (A_9B_2). *Eur. J. Mineral.*, **3**, 793-808.

Grew, E.S. (1996): Borosilicates (exclusive of tourmaline) and boron in rock-forming minerals in metamorphic environments. *Reviews in Mineralogy*, **33**, 387-502.

Grew, E.S., McGee, J.J., Yates, M.G., Peacor, D.R., Rouse, R.C., Huijsmans, J.P.P., Shearer, C.K,, Wiedenbeck, M., Thost, D.E., Su, S.-C. (1998): Boralsilite ($Al_{16}B_6Si_2O_{37}$): A new mineral related to sillimante from pegmatites in granulte-facies rocks. *Amer. Mineral.*, **83,** 638-651.

Grigoriev, A.P. & Brovkin, A.A. (1969): Study of the binary join sellaite-kotoite in the system MgO-MgF_2-B_2O_3. *Dokl. Akad. Nauk SSSR*, **186**, 1387-1390 (in Russian).

Mandarino, J.A. (1979): The Gladstone-Dale relationship. Part III: Some general applications. *Canad. Mineral.*, **17**, 71-76.

Nickel, E.H. & Grice, J.D. (1998): The IMA Commission on New Minerals and Mineral Names: procedures and guidelines on mineral nomenclature, 1998. *Canad. Mineral.*, **36,** 913-926.

Nickel, E.H. & Mandarino, J.A. (1987): Procedures involving the IMA Commission on New Minerals and Mineral Names and guidelines on mineral nomenclature. *Amer. Mineral.*, **72**, 1031-1042.

Niven, M.L., Waters, D.J., Moore, J.M. (1991): The crystal structure of werdingite, $(Mg,Fe)_2Al_{12}(Al,Fe)_2Si_4(B,Al)_4O_{37}$, and its relationship to sillimanite, mullite, and grandidierite. *Amer. Mineral.*, **76**, 246-256.

Peacor, D.R., Rouse, R.C., Grew, E.S. (1999): Crystal structure of boralsilite and its relation to a family of boroaluminosilicates, sillimanite, and andalusite. *Amer. Mineral.*, **84**, 1152-1161.

Pertsev, N.N. (1971): Paragenesis of boron minerals in magnesian skarns. Nauka, Moscow, 192 pp. (in Russian).

Pöter, B., Werding, G., Schreyer, W., Bernhardt, H.-J. (1998): Synthesis and properties of the new borosilicate mineral boralsilite. *Berichte Deutsche Mineralogische Gesellschaft, Beih. z. Eur. J. Mineral.*, Vol. **10**, No. 1, 220.

Pouchou, J.L. & Pichoir, F. (1984): A new model for quantitative x-ray miicroanalysis. Part I: Application to the analysis of homogeneous sample. *Rech. Aérosp.*, **1984**-3, 13-18.

Rudnev, V.V. (1996): Monoclinic iron-magnesium oxyborates of the hulsite isomorphic series. (in Russian) *Zap. Vser. Mineral. Obsh.*, No. 1, 89-1099.

Schreyer, W., Pertsev, N.N., Armbruster, T. Bernhardt, H.-J., Medenbach, O. (2002): Two potentially new borate minerals in a kotoite-bearing marble from Eastern Siberia. Abstracts 18th Gen. Meeting Int'l Mineral. Assoc., p. 205.

Sheldrick, G.M. (1997a): SHELXS-97. A computer program for crystal structure determination. University of Göttingen, Germany.

– (1997b): SHELXL-97. A computer program for crystal structure refinement. University of Göttingen, Germany.

Werding, G. & Schreyer, W. (1992): Synthesis and stability of werdingite, a new phase in the system MgO-Al_2O_3-B_2O_3-SiO_2 (MABS), and another new phase in the ABS-system. *Eur. J. Mineral.*, **4**, 193-207.

–, – (1996): Experimental studies on borosilicates and selected borates. *Reviews in Mineralogy*, **33**, 117-163.

Woodford, D.T., Sisson, V.B., Leeman, W.P. (2001): Boron metasomatism of the Alta stock contact aureole, Utah: Evidence from borates, mineral chemistry, and geochemistry. *Amer. Mineral.*, **86**, 513-533.

Yvon, K., Jeitschko, W., Parthe, E. (1977): LAZYPULVERIX, a computer program, for calculating X-ray and neutron diffraction powder patterns. *J. Appl. Cryst.*, **10**, 73-74.

Received 14 January 2003
Modified version received 20 May 2003
Accepted 13 June 2003